

Silicon nitride based nanocomposites produced by two different sintering methods

O. Tapasztó^{a,*}, P. Kun^a, F. Wéber^a, G. Gergely^a, K. Balázsi^a, J. Pfeifer^a,
P. Arató^a, A. Kidari^b, S. Hampshire^b, C. Balázsi^a

^a Research Institute for Technical Physics and Materials Science, 1121 Budapest, Konkoly-Thege út 29–33, Hungary

^b Materials and Surface Science Institute, University of Limerick, Limerick, Ireland

Received 29 October 2010; received in revised form 19 April 2011; accepted 4 May 2011

Available online 12 June 2011

Abstract

This research explores the use of a variety of carbon nanostructures as reinforcing agents for Si_3N_4 matrix composites. We have chosen highly promising families of carbon materials: multiwall, singlewall carbon nanotubes (MWCNTs, SWCNTs), graphene, carbon black nanograins and graphite micrograins for use as fillers. These materials were dispersed with a concentration of 3 wt% in silicon nitride matrices. A high efficiency attritor mill has also been used for effective dispersion of second phases in the matrix. In the present work the development of sintering processes (hot isostatic pressing (HIP) and spark plasma sintering (SPS)) has been performed to consolidate and tailor the microstructure of Carbon nanotube (CNT)-reinforced silicon nitride-based ceramic composites. The silicon nitride nanocomposite systems retained the mechanical robustness of the original systems. Elastic modulus measurements and micro-indentation investigations of the hardness and fracture toughness have been performed as well as scanning electron microscopy (SEM), transmission electron microscopy (TEM) and X-ray diffraction in order to characterize the composites produced by the two sintering methods.

© 2011 Elsevier Ltd and Techna Group S.r.l. All rights reserved.

Keywords: A. Hot isostatic press; B. Composites; D. Si_3N_4 ; Spark plasma sintering

1. Introduction

Carbon nanotubes (CNTs) have been shown to possess exceptional physical properties and therefore it is expected that their addition can improve the mechanical, thermal and electrical performance of polymer, metal and ceramic matrices [1–5]. An important factor is the type and quality of the carbon nanotubes used as reinforcing agents [6]. Up to now, several types of carbon nanotubes with different properties have been prepared using different synthesis methods [7,8].

When using conventional sintering techniques (hot pressing, hot isostatic pressing (HIP)), characterized by extended holding times at very high temperatures and pressures, the deterioration of the CNTs can easily occur [9,10]. In contrast, with spark plasma sintering (SPS) it is possible to prepare fully densified composites at lower temperatures and substantially shorter

holding times. This method has already been successfully applied to a wide range of ceramics (oxides, nitrides, carbides and their composites) [11–13], where a rapid densification could be achieved [14,15]. The SPS method is similar to a conventional hot pressing process, where the precursor powders are loaded in a die and a uni-axial pressure is applied during the sintering. However, instead of using an external heating source, an electrical current, which is typically a few thousands of amperes passes through the graphite die and the sample. Conduction along the die represents basically a resistance heating, while the conduction through the sample may generate breakdown, arcing, spark or plasma among powder particles that induce a fast densification process. By using the SPS method the densification of the samples without a considerable grain growth process can be achieved within a few minutes [15].

In this study we compare SPS with the conventional hot isostatic pressing method for Si_3N_4 /carbon nanostructure composite preparation. The morphological, structural and mechanical characteristics of the composites prepared by the two methods are presented and discussed.

* Corresponding author. Tel.: +36 1 392 2222x1315; fax: +36 1 392 2226.

E-mail address: o.tapaszto@mfa.kfki.hu (O. Tapasztó).

2. Experimental procedure

Si_3N_4 (Ube, SN-ESP) has been used as starting powder, whereas as sintering aids we used the following powders: AlN (H.C. Starck, grade C), Al_2O_3 (Alcoa, A16) and Y_2O_3 (H.C. Starck, grade C). The powder mixtures were milled in ethanol in an attritor mill (4000 rpm, 5 h). After milling the following carbon additions have been added to the batches: single- and multi-walled carbon nanotubes (SWCNT -Nanocyl- and MWCNT -Szege University), exfoliated graphite (GR) and carbon black (CB).

Two different sintering methods were applied for sample preparation:

1. For *hot isostatic pressing* (HIP - ABRA type) the powder mixture was placed in an ethanol bath and sonicated for 1 h. After sonication, polyethylene-glycol (PEG) was added.

The batches were sieved through 150 μm mesh. Green samples were obtained by dry pressing at 220 MPa. An oxidation procedure was applied, at very low heating rates up to 400 $^{\circ}\text{C}$, to eliminate the PEG. The sintering procedure was performed at 1700 $^{\circ}\text{C}$ and 20 MPa pressure applied for 3 h in high-purity nitrogen gas, and using BN embedding powder. The heating rate was not exceeding 25 $^{\circ}\text{C}/\text{min}$. The dimensions of the as-sintered specimens were 3.5 mm \times 5 mm \times 50 mm.

2. *Spark plasma sintering* was performed in vacuum using a Dr. Sinter 2050 (Sumitomo Coal Mining) apparatus. The powder mixtures were loaded in cylindrical carbon dies with an inner diameter of 10 mm. The samples were heated via a pulsed d.c. current that assured 100 $^{\circ}\text{C}/\text{min}$ heating rate for all of the experiments. The temperature was automatically raised to 600 $^{\circ}\text{C}$ over a period of 3 min, and from this point onwards it was monitored and regulated by an optical pyrometer focused on the surface of the die. A uniaxial pressure of either 50 MPa or 100 MPa was applied from the start to the end of the sintering cycle. Short holding times were used, from 3 to 5 min. The set-up allowed a cooling rate of about 400 $^{\circ}\text{C}/\text{min}$ in the temperature range 1650–1000 $^{\circ}\text{C}$. Samples with \varnothing 10 mm \times 5 mm were obtained.

The structure of nanocomposite powders was investigated by conventional transmission electron microscopy (TEM) using a Philips CM-20 (200 kV) microscope. The elemental compositions were measured by Ge detector NORAN EDS (Energy Dispersive Spectrometer), attached to the CM-20 microscope. The starting powder samples were prepared on Cu grid with thin carbon tape for TEM and EDS measurements. The phase analyses of the sintered samples have been performed using a Philips PW 1050 diffractometer. The morphology of the solid products was studied by field emission scanning electron microscope, LEO 1540 XB FESEM.

Elastic modulus measurements and micro-indentation investigations of the hardness and fracture toughness have been performed. Vickers hardness HV10 was measured on a hardness tester (KS Prüftechnik) applying a load of 10 Kp for 10 s. The fracture toughness was calculated according to the Anstis-formula [16].

For HIP samples, the elastic modulus was determined by a bending test with spans of 40 and 20 mm while for SPS samples it was determined by an ultrasonic method [17].

3. Results and discussion

Starting powder mixtures consisted of $\alpha\text{-Si}_3\text{N}_4$, Al_2O_3 , Y_2O_3 grains and 3 wt% of carbon nanostructure as addition to batches. As revealed by TEM analysis, after milling by high efficient attritor, the ceramic powder comprised of ~ 200 nm crystallites and dispersed carbon nanostructures (Fig. 1a). In Fig. 1a the dispersed multi-walled carbon nanotubes in the ceramic powder mixture may be observed. The nanotube radius is ~ 50 nm. In Fig. 1b the dispersed exfoliated graphite sheets can be seen, whereas in Fig. 1c the separated MWCNTs and carbon black particles spread among the starting ceramic powder are shown.

In Table 1 the results of EDS measurements are shown taken from two separate locations within the powder sample containing MWCNTs. Zirconia contamination may be observed and is a result of high energy milling. A copper grid with thin carbon tape was used for TEM sample preparation and therefore carbon was not measured.

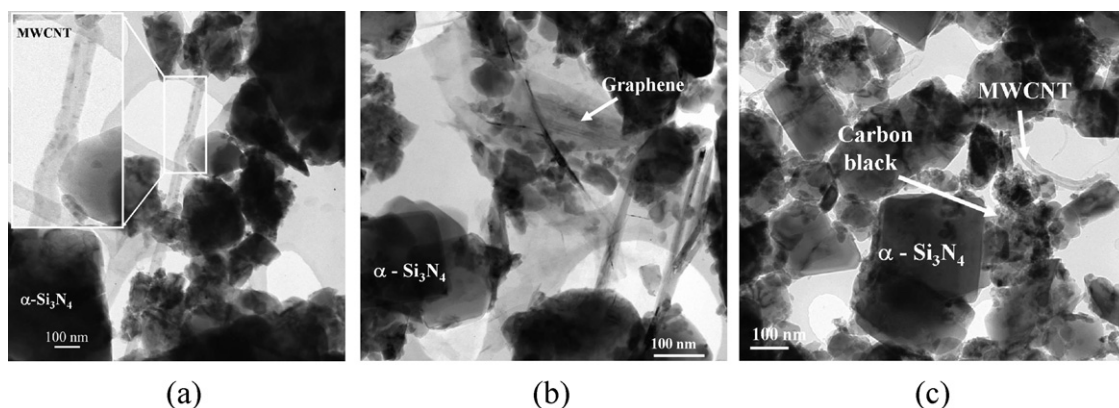


Fig. 1. Transmission electron microscopy of starting nanocomposites powders showing the dispersion of carbon nanostructures in starting powder. a) with MWCNTs, b) with graphene, c) with 2 wt% MWCNTs and 1 wt% CB.

Table 1

EDS results taken from two separate locations in powder mixtures with additions of carbon nanostructured particles.

Element	3 wt% MWCNT		3 wt% Graphene		2 wt% MWCNT and 1 wt% CB	
	1.location	2.location	1.location	2.location	1.location	2.location
Si (at.%)	46.54	60.62	42.61	56.90	59.47	37.71
N (at.%)	18.44	21.38	12.35	17.24	21.27	18.67
O (at.%)	6.99	11.78	7.24	11.81	11.39	8.39
Al (at.%)	2.92	3.81	2.52	6.22	4.88	2.35
Y (at.%)	0.84	0.57	2.23	2.45	1.16	0.87
Zr (at.%)	2.24	1.85	2.45	3.06	1.83	1.56

In order to investigate the morphology of the prepared composites, scanning electron microscopy (SEM) investigation of the fracture surfaces of silicon nitride composites have been performed as shown in Fig. 2. As apparent from the micrographs the MW- and SW-CNTs have been preserved in the Si_3N_4 matrices in both methods. Although it is expected that the carbon nanotubes are less damaged during the SPS process, SEM measurements are not conclusive enough to unequivocally prove this. Nevertheless, they provide important information about the distribution of the carbon nanostructures in the ceramic matrices. According to SEM investigations the nanotubes are mainly located in inter-granular locations and in some cases incorporated into silicon nitride grains.

In composite preparation the dispersion of fillers is a crucial but a very challenging task. Although an efficient milling process of CNT-containing powder mixtures has been performed, the agglomeration of the carbon nanostructures

still occurs, as can be seen in Fig. 2. The interconnected nanotube networks seen in the SEM images are also responsible for the enhanced electrical conductivity of the prepared composites (as shown in Fig. 2a) [18].

In order to investigate the phase composition as a function of the preparation methods, X-ray diffraction measurements have been performed. The results are presented in Fig. 3.

The diffractometer traces of the HIP samples reveal that after sintering the silicon nitride composite has $\beta\text{-Si}_3\text{N}_4$ phase as its main component ($\beta\text{-Si}_3\text{N}_4$, JCPDS-PDF 33-160). By contrast samples sintered using the SPS method mainly consists of $\alpha\text{-Si}_3\text{N}_4$ (JCPDS-PDF 41-360), while the $\beta\text{-Si}_3\text{N}_4$ phase is present in small quantities. $\text{ZrO}_{1.96}$ (JCPDS-PDF 81-1546), contamination from the milling balls and agitator liners can be recognized.

To compare the mechanical properties of the composites prepared using the two methods, a series of mechanical

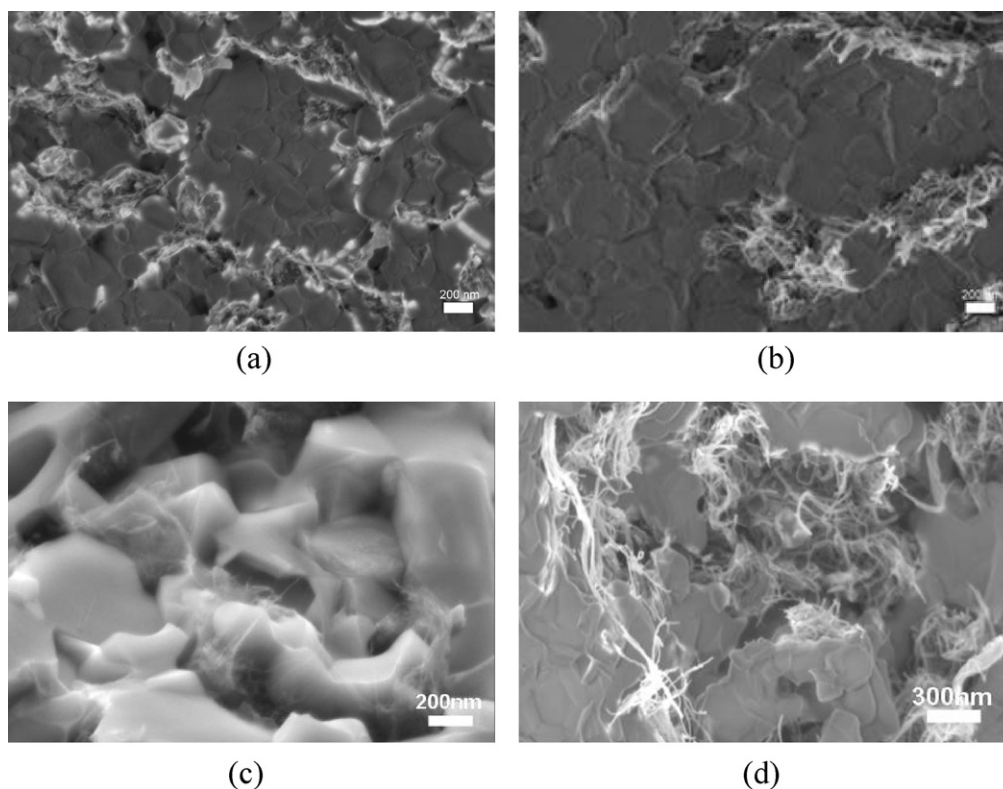


Fig. 2. SEM micrographs of fracture surfaces of Si_3N_4 composite prepared using SPS (a, b) and using HIP method (c, d) containing 3% SWCNT (a, c) and 3% MWCNT (b, d), respectively.

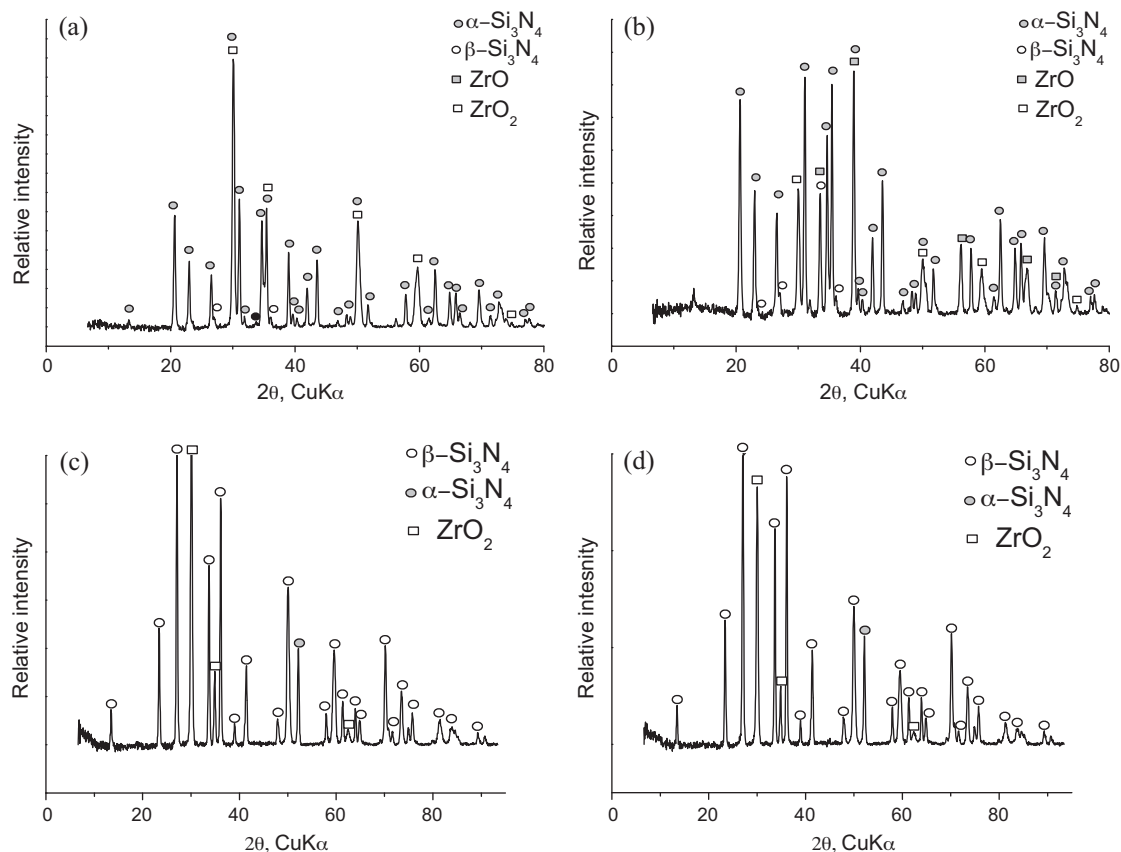


Fig. 3. X-ray diffractograms of SPS (a, b) and HIP (c, d) samples, containing 3 wt% SWCNTs (a, c) and 3 wt% MWCNTs (b, d), respectively.

measurements were performed. The results of the elastic modulus measurements and micro-indentation investigations of the hardness and fracture toughness are summarized in Table 2.

The results of elastic modulus, hardness and fracture toughness measurements for different carbon filler additions are graphically summarized in Fig. 4.

As apparent from Fig. 4a the samples prepared with SPS method show elastic modulus values enhanced by 10–20% for all types of carbon additions as compared to the samples prepared by the HIP method. In contrast the fracture toughness measurements shown in Fig. 4b display higher values for samples prepared by the HIP method for all carbon additions excepting SWCNTs.

The most significant improvement was observed in the hardness of the SPS sintered samples as compared to the HIP samples, showing values 30–40% higher in the former case.

This is even more spectacular for the case of the SPS sintered MWCNTs sample, where the measured hardness values exceed the ones of the reference sample.

The observed differences in the mechanical properties of the samples prepared by different sintering methods have complex processes at their origin. Here we would like to emphasize two factors, which most certainly play an important role in the properties of the resulting composites. (1) The effect of different sintering kinetics on the phase transformation of the silicon nitride matrix, which is clearly reflected also in the final phase composition of the samples (SPS sintered samples mainly consist of alpha Si_3N_4 , while HIP sintered samples predominantly contain beta Si_3N_4 grains). (2) The effect of holding times at high temperatures on the structure (degradation) of the carbon fillers. It is known, that both carbon nanotubes and graphene can be damaged during long exposures

Table 2
Mechanical parameters of Si_3N_4 based composites.

Sample	Composition	HIP			SPS		
		Young modulus (GPa)	Kic ($\text{MPa}/\text{m}^{0.5}$)	HV (GPa)	Young modulus (GPa)	Kic ($\text{MPa}/\text{m}^{0.5}$)	HV (GPa)
1	3%SW	155.7	2.65	8.12	226.14	3.51	16.97
2	2%MW-1%CB	187.66	4.43	9.57	247.50	3.12	12.15
3	3%MW	157.66	4.5	10.41	231.74	3.35	18.73
4	100% Si_3N_4	261.33	4.84	15.17	297.1	3.97	17.89
5	3%CB	223	4.67	10.66	268.87	4.41	17.09
6	3%GR	214	4.29	12.6	227.37	3.24	17.37

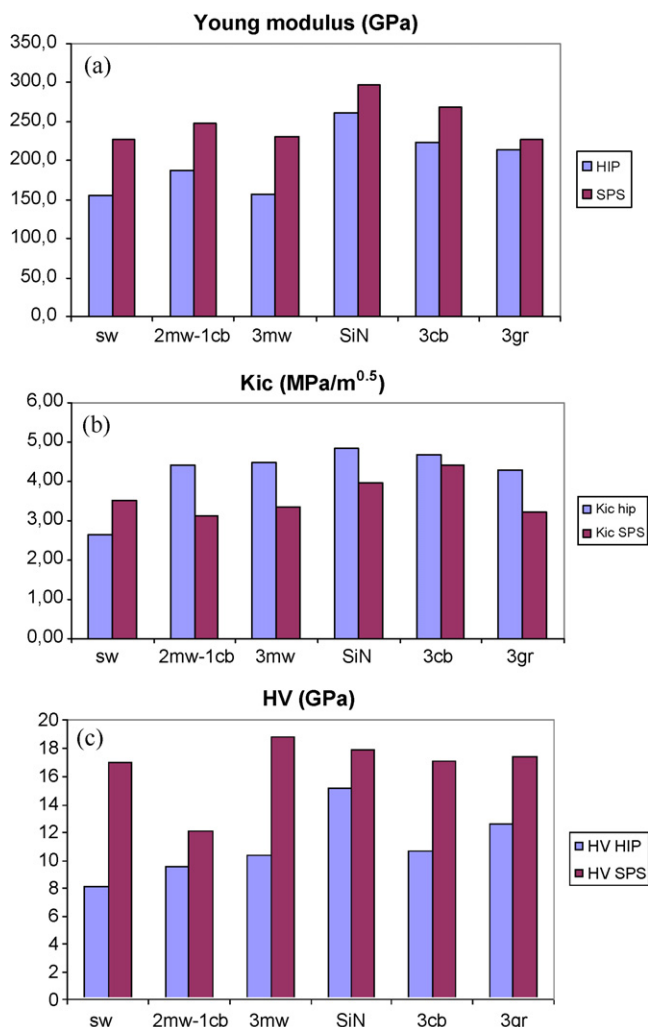


Fig. 4. Comparative diagrams of different mechanical properties (elastic modulus-a, indentation toughness-b and hardness-c) of reinforced silicon nitride composites with different types of carbon addition, prepared using HIP (blue) and SPS (plum) method.

to high temperatures, whereupon their intrinsic mechanical properties can substantially decay. In this sense, the short holding times of the SPS method are expected to better preserve the excellent mechanical properties of the filler phase.

4. Conclusions

In this work we compared the structure and mechanical properties of Si_3N_4 composites reinforced with several types of carbon nanostructures and prepared by two different sintering methods. A series of mechanical measurements have been made and analyses using scanning electron microscopy as well as X-ray diffraction have been carried out in order to characterize the structure and properties of the resulting composites. According to these measurements composites prepared using different sintering methods possess strikingly different structural and mechanical properties, which can be exploited in different types of applications. Namely, while samples sintered by the spark plasma sintering method mainly

consist of $\alpha\text{-Si}_3\text{N}_4$ and so are harder and stiffer, the composites prepared by hot isostatic pressing are characterized by $\beta\text{-Si}_3\text{N}_4$ grains and provide tougher composites.

Acknowledgements

Thanks to Dr. Z.E. Horváth and Dr. A.L. Tóth for XRD and SEM measurements. Financial support of OTKA 76181 and 63609 is acknowledged.

References

- [1] S. Rochie, Carbon nanotubes: exceptional mechanical and electrical properties, *Ann. Chim. Sci. Mater.* 25 (2000) 529–532.
- [2] E.T. Thostenson, Z. Ren, T.W. Chou, Advances in the science and technology of carbon nanotubes and their composites: a review, *Compos. Sci. Technol.* 61 (2001) 1899–1912.
- [3] S. Pasupuleti, R. Peddetti, S. Santhanam, K.-P. Jen, Z.N. Wing, M. Hecht, J.P. Halloran, Toughening behavior in a carbon nanotube reinforced silicon nitride composite, *Mater. Sci. Eng. A* 491 (1–2) (2008) 224–229.
- [4] J. Dusza, J. Morgiel, P. Tatarko, V. Puchy, Characterization of interfaces in ZrO_2 -carbon nanofiber composite, *Scripta Mater.* 61 (3) (2009) 253–256.
- [5] K. König, S. Novak, A. Iveković, K. Rade, D. Meng, A.R. Boccaccini, S. Kobe, Fabrication of CNT-SiC/SiC composites by electrophoretic deposition, *J. Eur. Ceram. Soc.* 30 (5) (2010) 1131–1137.
- [6] M.I. Osendi, F. Gautheron, P. Miranzo, M. Belmonte, Dense and homogeneous silicon nitride composites containing carbon nanotubes, *J. Nanosci. Nanotechnol.* 9 (10) (2009) 6188–6194.
- [7] Z. Konya, I. Vesselényi, K. Niesz, A. Kukovecz, A. Demortier, A. Fonseca, J. Delhalle, Z. Mekhalif, J.B. Nagy, A.A. Koos, Z. Osvath, A. Kocsy, L.P. Biro, I. Kiricsi, Large scale production of short functionalized carbon nanotubes, *Chem. Phys. Lett.* 360 (2002) 429–435.
- [8] L.P. Biro, Z.E. Horvath, L. Szalmas, K. Kertesz, F. Weber, G. Juhasz, G. Radnóczi, J. Gyulai, Continuous carbon nanotube production in under-water AC electric arc, *Chem. Phys. Lett.* 372 (2003) 399–402.
- [9] E. Flahaut, A. Peigney, Ch. Laurent, Ch. Marliere, F. Chastel, A. Rousset, Carbon nanotube-metal-oxide nanocomposites: microstructure, electrical conductivity and mechanical properties, *Acta Mater.* 48 (2000) 3803–3812.
- [10] Cs. Balazsi, Z. Konya, F. Weber, L.P. Biro, P. Arato, Preparation and characterization of carbon nanotube reinforced silicon nitride composites, *Mater. Sci. Eng. C* 23 (6–8) (2003) 1133–1137.
- [11] M. Nygren, Z. Shen, On the preparation of bio-, nano- and structural ceramics and composites by spark plasma sintering, *Solid State Sci.* 5 (2003) 125–131.
- [12] Z. Shen, H. Peng, J. Liu, M. Nygren, Conversion from nano- to micron-sized structures: experimental observations, *J. Eur. Ceram. Soc.* 24 (2004) 3447–3452.
- [13] R.S. Dohedoe, G.D. West, M.H. Lewis, Spark plasma sintering of ceramics, *Bull. Eur. Ceram. Soc.* 1 (2003) 19–24.
- [14] E.L. Corral, J. Cesarano, A. Shyam, E. Lara-Curzio, N. Bell, J. Stuecker, N. Perry, M. DiPrima, Z. Munir, J. Garay, E.V. Barrera, Engineered nanostructures for multifunctional single-walled carbon nanotube reinforced silicon nitride nanocomposites, *J. Am. Ceram. Soc.* 91 (10) (2008) 3129–3137.
- [15] J.R. Groza, A. Zavaliangos, Sintering activation by external electrical field, *Mater. Sci. Eng.* 287 (2000) 171–177.
- [16] G.R. Anstis, P. Chantikul, B.R. Lawn, D.B. Marshall, A critical evaluation of indentation techniques for measuring fracture toughness: I, direct crack measurements, *J. Am. Ceram. Soc.* 64 (1981) 533–538.
- [17] A. Díaz, S. Hampshire, J.-F. Yang, T. Ohji, S. Kanzaki, Comparison of mechanical properties of silicon nitrides with controlled porosities produced by different fabrication routes, *J. Am. Ceram. Soc.* 88 (2005) 698–706.
- [18] C. Balázs, B. Fényi, N. Hegman, Z. Kövér, F. Weber, et al. Composites B 37 (2006) 418.